JOC The Journal of Organic Chemistry

Article

pubs.acs.org/joc

Asymmetrically Substituted and π-Conjugated 2,2′-Bipyridine Derivatives: Synthesis, Spectroscopy, Computation, and Crystallography

Ramakrishna Bodapati, Monima Sarma, Arunkumar Kanakati, and Samar K. Das*

School of Chemistry, University of Hyderabad, Central University P.O., Hyderabad 500 046, India

Supporting Information

ABSTRACT: A new series of monosubstituted styryl- and bistyryl-2,2′-bipyridine luminophores (compounds **16**−**23**) have been synthesized via Horner−Wadsworth−Emmons reaction involving a monophosphonate and donor aromatic aldehydes. In the title chromophores, the amino donors are varied between acyclic and cyclic while the alkoxy donors are varied in terms of their number and position. The absorption maxima of these chromophores shift predominantly due to intramolecular charge transfer (ICT) between different donor and acceptor moieties. The title donor−acceptor molecules exhibit intense fluorescence in solution at room temperature, and their emissive behavior has been found to be highly sensitive to solvent polarity. The fluorescence spectra and quantum yields of all the chromophores were recorded in four different solvent media, and the chromophores **16**, **17**, **19**, and **21** exhibit fluorescence in the solid state too. The influence of the nature and position of the donor functionalities in the conjugated backbone of the bipyridine moiety on the electronic absorption properties of the title chromophores (**16**−**23**) has been demonstrated, which has further been corroborated by DFT and TD-DFT computation both in gas phase and in solution phase. The crystal structure of compound **18** has been described as a representative member of the family (**16**−**23**).

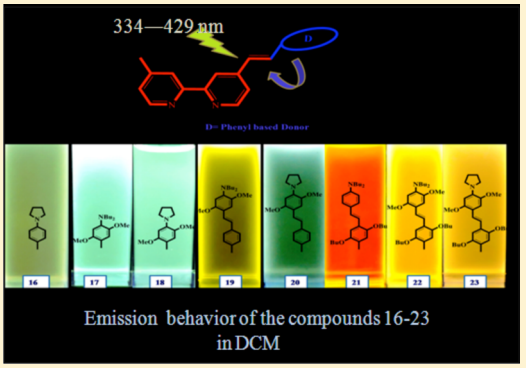

INTRODUCTION

In recent years, π-conjugated functional materials have attracted a great deal of attention by virtue of their enormous applications in organic light emitting diodes (OLEDs),[1] nonlinear optics (NLOs),[2] electrogenerated chemiluminescence (ECL),[3] dye-sensitized solar cells (DSSCs),[4] fluorescent sensors,[5] etc. Among the diverse classes of organic π-conjugated systems, the push−pull chromophores with donor and acceptor moieties have generated a lot of interest since their optical properties can be tuned judiciously over a wide range simply by varying the donor or acceptor moieties. The fundamental type of interaction in such molecules generally occurs by an intramolecular charge-transfer (ICT) between the donor (D) and the acceptor (A), thereby tuning the HOMO−LUMO energy gap. In this regard, the heteroaromatic DA-type fluorescent probes can be considered as potential candidates, and among the diverse classes of DA-type building blocks, 2,2′-bipyridines act as very promising building blocks because of their ability to tune their optical properties very easily either by extending the conjugation or by introducing an assorted class of donor end-capped functionalities, or via a metal complexation. As the orbital energy of the lowest unoccupied molecular orbital (LUMO) of pyridine is lower than that of benzene (due to the presence of ring nitrogen atom), pyridine is a good electron accepting mesomeric unit, and thus, suitable push−pull chromophores can be designed and synthesized simply by end-capping the pyridine ring with various donor moieties.

The 2,2′-bipyridine derivatives are endowed with an enriched coordination chemistry and have received much attention because they can readily form complexes with transition metals, where they can bind with metals both by σ-molecular orbitals of the electron-donating nitrogen atoms and by electron accepting π-molecular orbitals.[6] The resulting metal complexes of such extended π-conjugated systems are very stable due to the formation of a five membered ring and are known to be excellent candidates for studying nonlinear optical properties. It has been reported by various research groups that 2,2′-bipyridine derivatives are known to complex metals in square-planar, tetrahedral, and octahedral coordination geometries and that the second-order nonlinear response of such π-conjugated systems is increased on coordination to a metal center.[7]

Zyss et al. reported the octupolar nonlinearity of $[Ru(bpy)_3]^{2+}$ complex ion;[8] later, abundant octupoles featuring the 4,4′-π-conjugated 2,2′-bipyridine derivatives were reported.[9] Such π-conjugated systems can also be used as antenna fragments in the TiO_2 anchoring heteroleptic ruthenium complexes, which come into competition with the silicon junction semiconductors so as to harvest solar energy. In recent years, there have been a growing number of reports containing π-conjugated ligands and their coordination complexes. For instance, Odobel and co-workers reported that heteroleptic

Received: October 9, 2015

DOI: 10.1021/acs.joc.5b02345
J. Org. Chem. XXXX, XXX, XXX−XXX

Chart 1. Molecules Synthesized and Studied in the Present Work

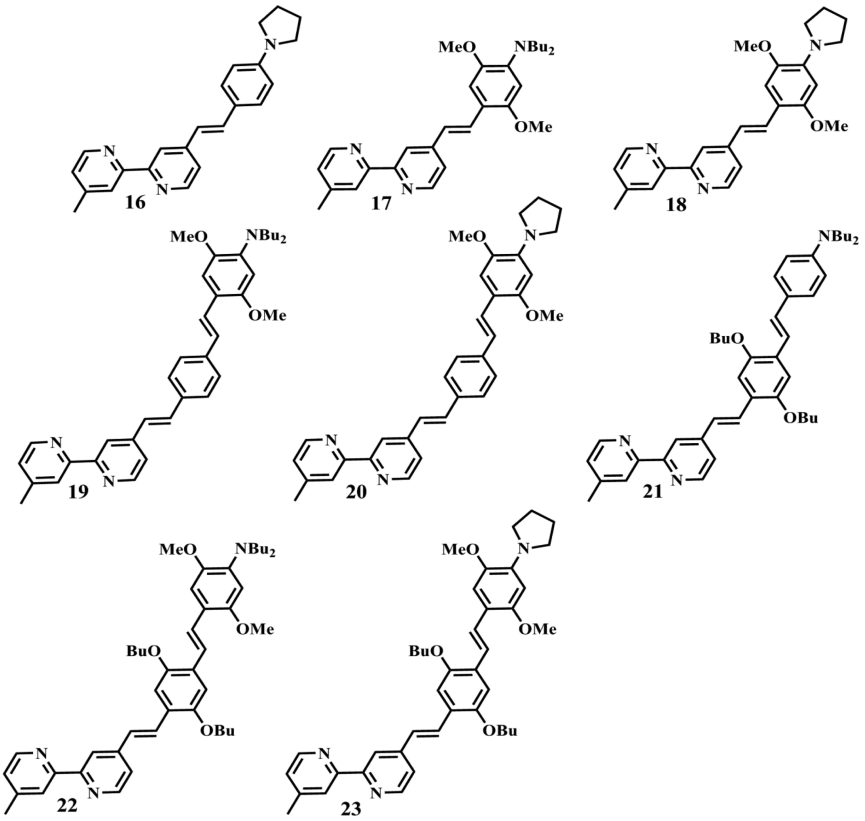

copper−polypyridine complexes display impressive power conversion efficiencies (PCEs) and thus could be used as efficient sensitizers in dye-sensitized solar cells.[10] Dragonetti et al. showed that cyclometalated Ir(III) complexes bearing different substituted 2-phenylpyridines act as interesting second-order NLO chromophores.[11] In a recent review, Bozec and Guerchais have accounted how new chromophores could be designed by combining dithienylethene (DTE)-based bipyridine ligands with different metallic fragments and studied both NLO and luminescence properties of the multi-photochromophoric materials.[12] Also, recently, the one- and two-photon absorption and emission properties of an oligo-(phenylenethienylene) series have been demonstrated by Nair et al.; this study revealed that increasing oligomer length results in only a slight shift of the two-photon absorption band with a drastic increase of two-photon absorption cross section.[13] Zhou and co-workers reported that 2,2′-bipyridine derivatives containing aza-crown ethers exhibit large two-photon absorption cross sections and their applicability for biomedical imaging.[14]

However, the π-conjugated bipyridine derivatives reported to date are substituted either symmetrically or unsymmetrically with identical donor functionalities. In our previous report,[15] we have discussed a series of symmetrically substituted heterodonor systems, containing a series of *styryl*- and *bistyryl*-2,2′-bipyridine luminophores, end-capped with alkoxy and amino donor functionalities having D−π−A−A−π−D (D = donor, A = acceptor) archetype. We have shown how simple modification of the π-skeleton of such dye molecules modulates their fluorescence behavior, and we have also described the diverse photophysical aspects on changing the amino donor from open chain dibutylamino (e.g., **MS 4**) to the cyclic pyrrolidine donor (e.g., **MS 5**).[15] All these reported compounds were found to exhibit high fluorescence quantum yields in solution state, and we also comprehended the modulating effect of the position, nature, and number of donor functionalities on the optical properties of such π-conjugated molecules by DFT and TD-DFT computational studies. The results obtained with the symmetrically substituted hetero-donor π-conjugated bipyridine derivatives inspired us to explore the unsymmetrically substituted heterodonor systems by functionalizing one of the pyridine rings of the bipyridine moiety, keeping the methyl group intact on the other pyridine ring. In this article, we have described synthesis, characterization, and photophysical studies of eight asymmetrically substituted 2,2′-bipyridine luminophores (compounds **16**−**23**, Chart 1). Though the target molecules can be obtained via three different synthetic routes, in the present work, the Horner−Wadsworth−Emmons reaction (HWE) has been exclusively used to introduce electron-donating groups onto the bipyridine acceptor core unit because this protocol is known to give high yields in addition to the *E*-selectivity. All the synthesized chromophores have unsymmetrical A−A−π−D archetype, wherein the A−A unit represents the 2,2′-bypyridine acceptor core, which is attached to the different donor termini through π-conjugation (see Chart 1). We have investigated the solvatochromic behavior and all the chromophores (compounds **16**−**23**) exhibit bright fluorescence in solution at room temperature with large Stokes shift; interestingly, chromophores **16**, **17**, **19**, and **21** exhibit solid-state emission too. We have also performed computational analysis in the level of density functional theory (DFT) in solvent reaction field to analyze the influence of "nature" and "position" of donor functionalities on the geometrical and electronic parameters of the synthesized

DOI: 10.1021/acs.joc.5b02345
J. Org. Chem. XXXX, XXX, XXX−XXX

Scheme 1. Synthetic Route of A−A−π−D Bipyridine Chromophores

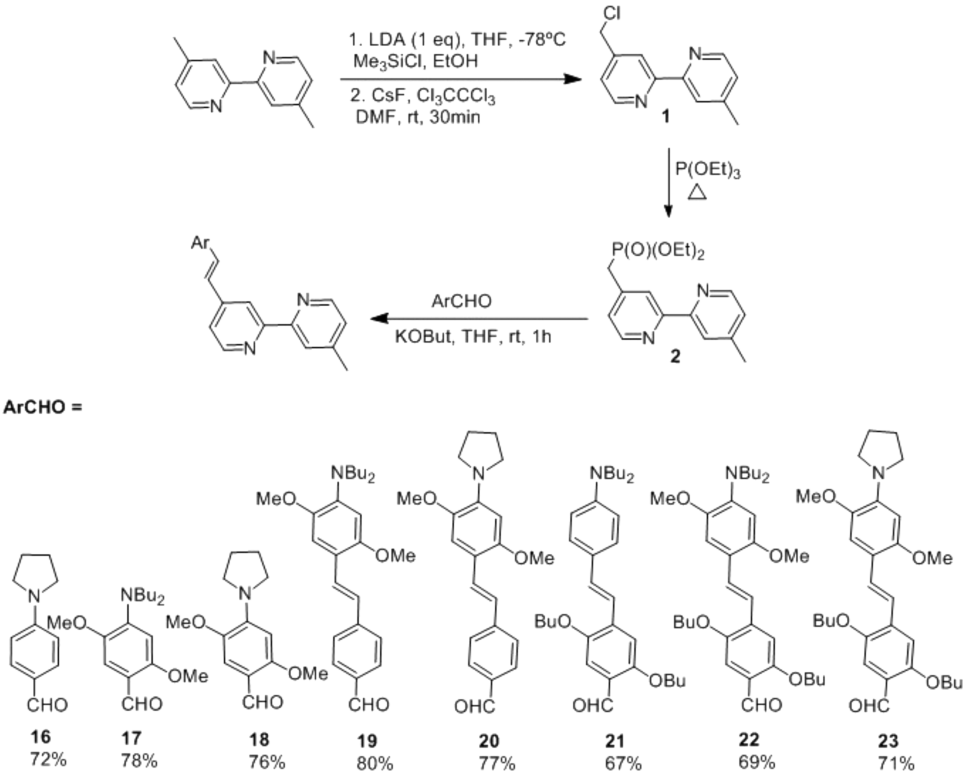

chromophores. One of the title compounds (chromophore **18**) has unambiguously been characterized by single crystal X-ray crystallography.

RESULTS AND DISCUSSION

Synthesis and Characterization. The bipyridine phosphonate precursor and appropriate aldehydes and their precursors were synthesized according to previous literature reports,[5−8,15,16] while the target molecules have been synthesized using an efficient HWE reaction protocol (Scheme 1). The advantages of the HWE reaction pathway over the conventional Wittig reaction are many-fold: the former has a good response with the stabilized yields and predominantly gives *E*-stereoselectivity of the olefinic double bond, generating a water-soluble phosphate salt which can easily be removed from the reaction mixture through an aqueous process. The great difficulty of separation of the Wittig byproduct, triphenylphosphine oxide, is thus largely ruled out in the HWE reaction. Consequently, this particular synthesis protocol has mainly been used for the synthesis of our target molecules. At first, the monochloromethyl derivative was synthesized by a method, developed by Smith and Fraser,[17] that involves usage of the base, LDA (instead of potassium *tert*-butoxide), which deprotonates the starting material by crucially controlling the amount of base used, thereby allowing in situ Knoevenagel-type reactions to be executed in order to achieve the unsymmetrically substituted chromophores. Thus, the proper selection of reaction conditions may effortlessly fabricate materials with desired symmetry. The HWE olefination, which enhances the yield of the phosphonate ester **2** as the reactive intermediate (Scheme 1), has received much acclamation for obtaining the π-conjugated bipyridine chromophores.

The open chain *N*,*N*-dialkylated anilines (**4a** and **4b**) were synthesized in good yields from anilines (**3a** and **3b**) by using suitable electrophiles via an intermolecular mode (Scheme S1). The corresponding cyclic (pyrrolidine) analogues (**6a** and **6b**, see Scheme S1) were synthesized by using 1,4-dibromobutane as the double electrophiles. The usage of 10% *N*-methylpyrrolidinone (NMP) in DMF as the solvent system affords the corresponding *N*,*N*-dialkylanilines in high yields, and thereafter, they were formylated using the Vilsmeier−Haack reaction which yielded excellent para-selectivity. In addition, the π-conjugated benzaldehydes (**10b−15b**, Scheme S2) with different substituents were obtained via a two-step synthetic approach. The synthesized pull−push compounds containing the open donors (**17**, **19**, **21**, and **22**) are highly viscous liquids, while those with cyclic pyrrolidine ring donors (**16**, **18**, **20**, and **23**) are solids.

The molecular structures of all the chromophores (**16−23**) are determined through NMR (^{1}H and ^{13}C) and mass spectroscopy including CHN analysis. The pyridine-H$^{6,6'}$ protons, being largely deshielded by the adjacent electronegative nitrogen atom, resonate at the lowest field of the spectra while the pyridine-H$^{5,5'}$ protons, owing to their meta-orientation with respect to the nitrogen atom, resonate in the benzene region. The downfield shift of the pyridine-H$^{3,3'}$ protons compared to the pyridine-H$^{5,5'}$ protons can be attributed to the transoid-arrangement of the two pyridine rings in the relevant bipyridine chromophores.[18] No indication of the *Z*-isomer has been observed, and the vinylic C=C bonds are found to be in *E*-geometry, as indicated by the coupling constant (*ca.* $^3J_{HH}$ = 16 Hz).

Comparison of the ^{1}H NMR signals due to the aromatic protons of the open chain amino donor end-capped chromophore **17** (dibutylamino donor) and its cyclic analogue **18** (pyrrolidine donor) clearly shows that the signals due to the cyclic donor are more upfield shifted (H^{11} nucleus resonate at δ 6.2) as compared to the open chain donor (H^{11} nuclei resonate

DOI: 10.1021/acs.joc.5b02345
J. Org. Chem. XXXX, XXX, XXX−XXX

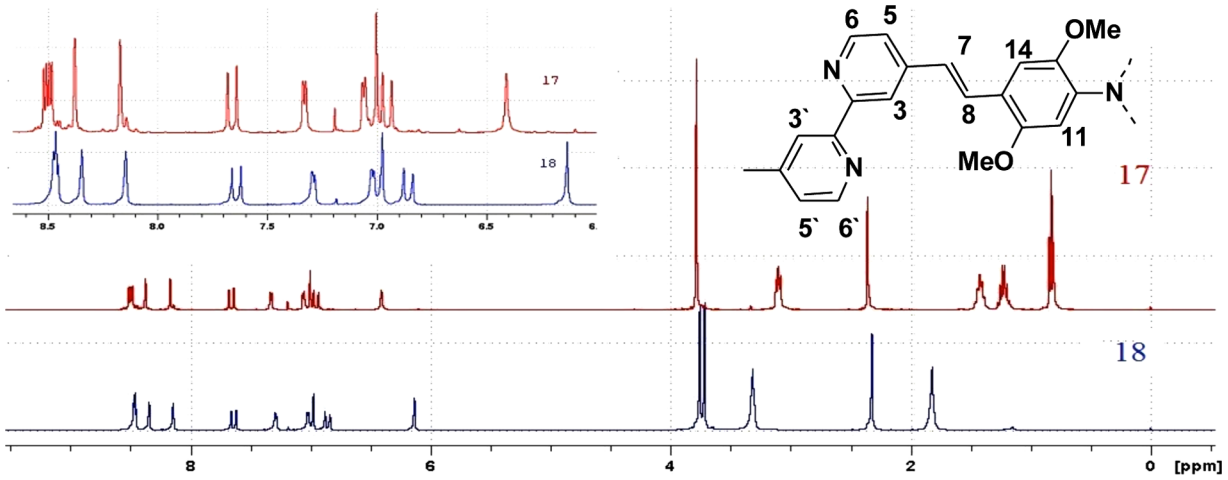

Figure 1. Difference in chemical shift of the proton adjacent to the amino donor (H^{11}) in **17** and **18**.

at δ 6.4), which is indicative of a more shielded environment around the relevant protons in the cyclic amino donor end-capped chromophores compared to open chain amino donor end-capped chromophore as shown in Figure 1. The electron-donating mesomeric effect of the amino groups makes the corresponding ortho-substituted phenyl rings more electron-rich, thereby exerting a greater shielding effect on the relevant protons (H^{11}). Thus, the better the delocalization of the amine lone pair into the phenyl ring, the greater will be the shielding effect on the relevant protons, thereby causing them to resonate at the upfield region of the relevant spectrum. In other words, it can be said that the pyrrolidine moiety has a greater electron-donating capability than the corresponding open chain amino donor, dibutylamine.

Optical Properties of Compounds (16−23) in Solution State. The photophysical properties of the synthesized compounds in solution phase were recorded in four different solvents, namely, toluene, dichloromethane (DCM), tetrahydrofuran (THF), and acetonitrile (MeCN), at room temperature, and the corresponding photophysical data are summarized in Table 1. The nature and position of the donor functionalities in the conjugated backbone of the bipyridine moiety and the polarity of the solvent media in which the compounds are solubilized have shown profound influence on the absorption and emission properties of all the investigated chromophores. The lowest energy absorption bands in the range of 330−430 nm in all the chromophores are due to an intramolecular $\pi \rightarrow \pi^*$ electronic transition from donor based molecular orbitals to acceptor molecular orbitals, which is affirmed owing to its sensitivity to solvent polarity. From the absorption spectra (Figure 2) and Table 1, it is quite evident that the compounds with pyrrolidine donors **18**, **20**, and **23** exhibit bathochromic shift by ≈10 nm compared to the compounds containing dibutylamino donors **17**, **19**, and **22** respectively; however, this trend is reversed for the pair of cyclic donor **20** (408 nm) and acyclic donor **19** (412 nm). Thus, the cyclic pyrrolidine ring has a greater donating capability compared to the open chain dibutylamino donor, which is consistent with NMR spectroscopy (vide supra). All the chromophores are highly fluorescent at room temperature, and when excited at the lowest energy absorption maxima, they exhibit excellent fluorescence behavior (Figure 2). The fact that the excited state of all the chromophores is more polar than the ground state is exemplified from the photophysical data obtained in various solvents (Table 1). On varying the solvent polarity from low to high, the shift in emission bands is found to be more profound than that in the absorption bands (Table

Table 1. Photophysical Data of All the A−A−π−D Bipyridine Chromophores 16−23

compound	solvent	λ_{max} (nm)	ε^a (M^{-1} cm^{-1})	λ_{em} (nm)	$\Phi_{em}{}^b$	$\Delta\bar{\nu}^c$ (cm^{-1})
16	toluene	325		408	0.20	6259
	DCM	334	50000	409	0.06	5490
	THF	333		413	0.07	5816
	MeCN	329		423	0.08	6754
17	toluene	388		476	0.17	4764
	DCM	395	49000	522	0.29	6159
	THF	393		506	0.31	5682
	MeCN	393		553	0.36	7362
18	toluene	402		482	0.16	4128
	DCM	407	45000	576	0.43	7208
	THF	404		516	0.27	5372
	MeCN	405		560	0.28	6834
19	toluene	402		560	0.78	7018
	DCM	412	31000	662	0.29	9166
	THF	407		637	0.59	8871
	MeCN	405		668	0.26	9721
20	toluene	411		571	0.63	6817
	DCM	408	45000	590	0.33	7864
	THF	402		627	0.43	8926
	MeCN	403		656	0.49	9569
21	toluene	419		561	0.37	6041
	DCM	428	45000	604	0.38	6808
	THF	418		602	0.46	7312
	MeCN	415		636	0.25	8373
22	toluene	380		483	0.56	5611
	DCM	381	37000	507	0.47	6522
	THF	380		514	0.51	6860
	MeCN	374		528	0.37	7798
23	toluene	420		543	0.45	5393
	DCM	429	34000	516	0.43	3930
	THF	418		512	0.47	4392
	MeCN	417		526	0.39	4969

[a] ε were measured in DCM solution. [b] Fluorescence: relative quantum yield of the compounds **16−23** was measured by using quinine sulfate (in 1 N H_2SO_4) as the reference (Φ_{em} = 0.545). [c] Stokes shift $\Delta\bar{\nu} = \bar{\nu}_{abs} - \bar{\nu}_{em}$.

DOI: 10.1021/acs.joc.5b02345
J. Org. Chem. XXXX, XXX, XXX−XXX

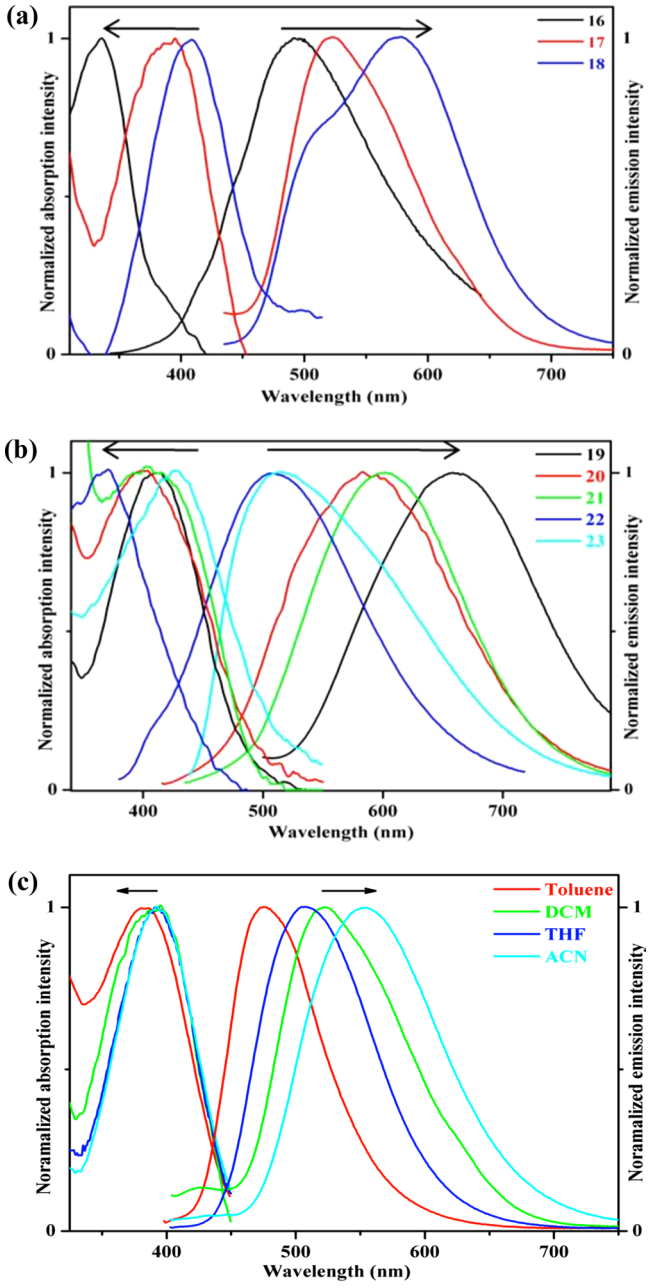

Figure 2. Normalized UV−vis absorption and emission spectra of compounds **16**−**18** (a) and compounds **19**−**23** (b), recorded in dichloromethane at room temperature. (c) Normalized UV−vis absorption and emission spectra of compound **17** (as representative one) showing the solvatochromic effect.

1 and Figure 2). Generally, the dipole character is boosted in the excited state S_1, when the electrons are excited from the highest occupied molecular orbital (HOMO) to the lowest unoccupied molecular orbital (LUMO). As a result, the solvents with high polarity tend to stabilize such polarized excited states by reorienting the solvent molecules so as to lower the energy of the system thereby leading to a red shift in the emission spectra.[19] This solvatochromic phenomenon is spectroscopically shown with compound **17** in Figure 2c, as a representative spectral change. The same solvatochromic phenomena for the rest of the compounds are displayed in Figures S2−S5.

The positions of the corresponding emission maxima are found to be independent of the excitation wavelength, which is in accordance with Kasha's rule, and it has been observed that, on increasing the conjugation length, the absorption and emission maxima are bathochromically shifted. For instance, when we compare the absorption and emission of **17** vs **19** or **18** vs **20** in DCM, it has been observed that the λ_{abs} and λ_{em} increase with increasing the conjugation length.

In a bid to check the variation in photophysical properties of the symmetrical chromophores[15] and the unsymmetrical chromophores (present study), we have also compared the photophysical properties of **MS 2** and **17**, **MS 3** and **18**, **MS 4** and **19**, **MS 5** and **20**, **MS 6** and **21**, **MS 7** and **22**, and **MS 8** and **23**, and the concerned data have been summarized in Table 2 along with their computationally obtained HOMO−LUMO gaps (the photophysical data of chromophores **MS 2** to **MS 8** have been taken from ref 15 in the present comparative discussion of the following paragraph).

Table 2. Comparison between Symmetrical[15] and Unsymmetrical (Present Work) Bipyridine Derivatives in Dichloromethane (DCM)

compd	λ_{abs} (nm)	λ_{em} (nm)	Φ_{em}	$\Delta\bar{\nu}$ (cm^{-1})	HOMO (eV)	LUMO (eV)	H−L (eV)
MS 2	399	533	0.20	6301	−6.204	−0.944	−5.26
17	395	522	0.29	6159	−6.139	−0.46	−5.67
MS 3	414	543	0.17	5738	−6.192	−0.934	−5.26
18	407	576	0.43	7208	−5.943	−0.413	−5.53
MS 4	413	644	0.37	8685	−6.342	−1.262	−5.08
19	412	662	0.29	9166	−6.013	−0.848	−5.17
MS 5	430	662	0.21	8150	−6.072	−1.229	−4.84
20	408	590	0.33	7864	−5.818	−0.820	−4.99
MS 6	442	598	0.65	5902	−6.214	−1.231	−4.98
21	428	604	0.38	6808	−5.944	−0.817	−5.13
MS 7	435	648	0.35	7556	−6.253	−1.247	−5.00
22	381	507	0.48	6522	−5.893	−0.824	−5.07
MS 8	448	660	0.23	7170	−6.018	−1.220	−4.80
23	429	526	0.40	4969	−5.718	−0.796	−4.92

Comparison between the chromophores (symmetrical and unsymmetrical) based on nature and position of the donor functionalities gives us some insight into the photophysical properties. In the case of cyclic donor systems, the absorption and emission bands in the unsymmetrical chromophores are blue-shifted with higher quantum yields compared to their symmetrical counterparts (except **18** emission) as shown in Table 2. However, in the acyclic donor systems, a different scenario has been observed. Though the absorption bands are blue-shifted on changing from symmetric to unsymmetric, there is an irregular trend observed in the emission behavior and, alternatively, solid-state fluorescence is observed in almost all of acyclic unsymmetrical compounds (except **22**). Furthermore, it has been observed that for the unsymmetrical compounds (present work), in which the alkoxy groups are attached to the ring with no amino group, the quantum yield of the chromophores is increased. For instance, in the acyclic systems, when the alkoxy group is shifted from second phenyl ring (**19**) to first phenyl ring (**21**), the quantum yield increases from 0.29 to 0.38 and the presence of two alkoxy groups in the system (**22**) further increases the quantum yield to 0.48. Again, the absorption band shows a bathochromic shift when the alkoxy group is shifted from second ring (**19**) to first ring (**21**) but

DOI: 10.1021/acs.joc.5b02345
J. Org. Chem. XXXX, XXX, XXX−XXX

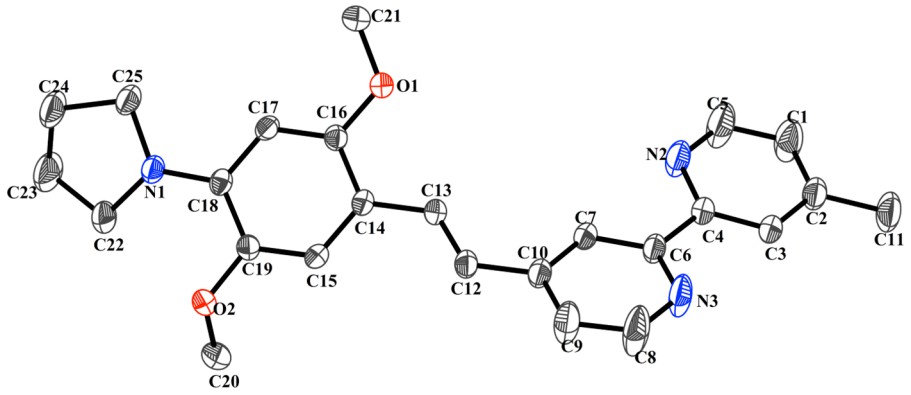

Figure 3. Thermal ellipsoidal plot of molecule **18** (30% probability). Hydrogen atoms have been omitted for clarity.

shows a hypsochromic shift with alkoxy groups on both rings; but surprisingly, there is a hypsochromic shift on the emission bands on altering the number and position of the alkoxy groups (from **19** to **21** to **22**).

Solid-State Emission of the Compounds. Of all the investigated chromophores, the chromophores **16**, **17**, **19**, and **21** show solid-state emission in addition to emission in solution (Figure S6). Solid-state UV/vis absorption spectra were recorded in diffuse reflectance mode. The samples were prepared in the form of KBr pellet (for homogeneity), and the reflectance spectra were converted to absorption spectra using the Kubelka–Munk function. The pertinent compounds absorb in the range 400–450 nm, and it is observed that there is a bathochromic shift in the absorption maxima in going from solution to solid state, which signifies the presence of intermolecular interactions between the molecules (might be due to *J* aggregation). This is indeed true because a representative crystal structure (compound **18**) shows *J* aggregation through intermolecular supramolecular interactions (vide infra, following section). When these chromophores are excited at their absorption maxima (Figure S6a), they exhibit emission at 618 nm, 628 nm, 536 nm, and 547 nm respectively as shown in Figure S6b. Even though the molecule **18** does not exhibit any emission at room temperature, it is one of the analogous members of the same family (compounds **16**–**23**) which should have similar intermolecular interactions as other members (which emit in the solid state) would have.

CRYSTALLOGRAPHY: CRYSTAL STRUCTURE OF COMPOUND 18

After purification by column chromatography was done, compound **18** solution in acetonitrile (MeCN) was kept for direct evaporation at room temperature, whereby brown color crystals, suitable for X-ray diffraction, were obtained after 2 days. Compound **18** crystallizes in monoclinic space group $P2_1/c$. The concerned asymmetric unit consists of the full molecule. The thermal ellipsoidal plot of the same is presented in Figure 3. The relevant crystal data and structure refinement parameters have been given in Table S1. The bond lengths and bond angles are presented in Tables S4 and S5 respectively. Interestingly in the crystal structure, the molecules undergo C–H···O and C–H···N intermolecular hydrogen bonding interactions leading to a three-dimensional supramolecular structure (Figure 4). This intermolecular supramolecular aggregation (*J* aggregation) justifies the bathochromic shift in the absorption maxima in going from solution to solid state (vide supra).

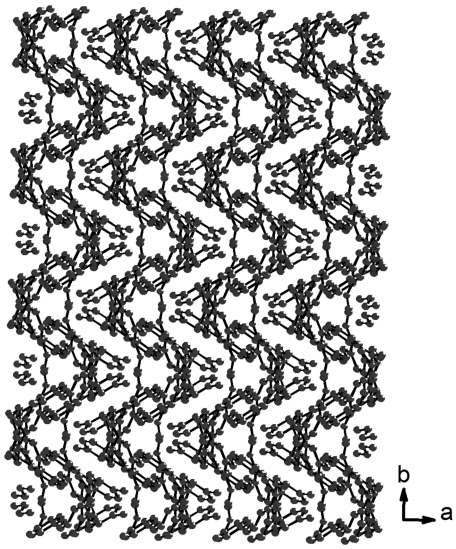

Figure 4. Molecular packing diagram in the crystal structure of compound **18**.

Theoretical Approach. In order to understand the trends in the behavior of vertical excitation (absorption maxima) shifts, HOMO–LUMO energy gaps etc., density functional theory (DFT) and time-dependent DFT (TD-DFT) were carried out on the compounds **16**–**23** using the Gaussian 09 program package.[20] The calculations were performed both in gas phase and solution phase using polarizable continuum model (C-PCM) applying self-consistent reaction field (SCRF) in DCM. The geometry of the target compounds was optimized at the level of exchange-correlation hybrid functional of CAM-B3LYP theory with the 6-31g(d,p) basis set. The optimized structures, identified as global minimum as the potential energy surfaces, were verified by the absence of any imaginary frequencies. The HOMO and LUMO frontier molecular orbitals (FMOs) of all the compounds **16**–**23** (via DFT computation) are presented in Figure 5, which indicate that an almost similar type of localization is observed for all the chromophores. The HOMO is constituted with the π-type combination of orbitals and is situated at the donor substituted phenyl rings and at the C=C bonds, while the LUMO is of π^*-type and is localized at the C=C bonds and the pyridine ring (see Figure 5). The modulation of energy for the four occupied (HOMO−3, HOMO−2, HOMO−1, HOMO) and four virtual (LUMO, LUMO+1, LUMO+2, LUMO+3) molecular orbitals are presented in Table 3 while the TD-DFT computed most

DOI: 10.1021/acs.joc.5b02345
J. Org. Chem. XXXX, XXX, XXX–XXX

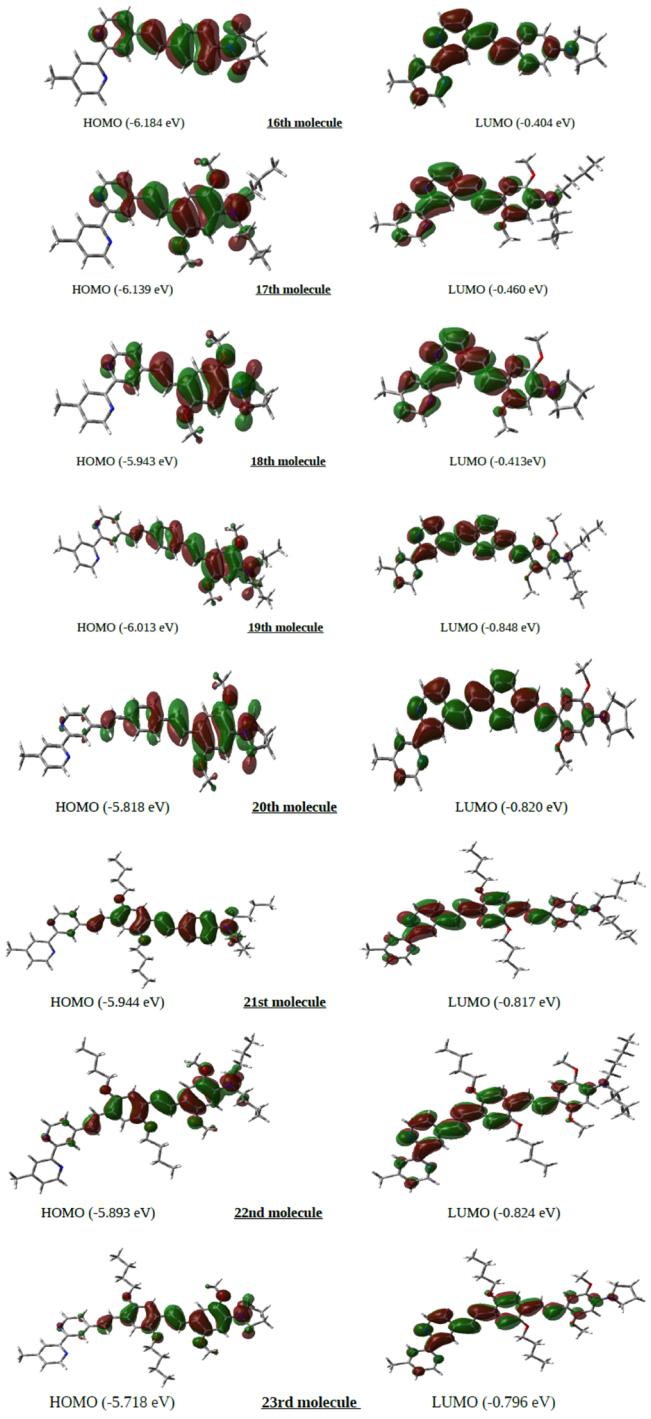

Figure 5. Isodensity plots of HOMO and LUMO frontier molecular orbitals of the synthesized molecules (**16**–**23**) as computed by the CAM-B3LYP/6-31g(d,p) level of theory (isodensity value = 0.02).

relevant $S_0 \rightarrow S_1$ vertical Franck–Condon electronic excitations between these energy levels (CAM-B3LYP/6-31g(d,p) in DCM) along with their associated oscillator strengths are shown in Table 4.

It is quite evident from Tables 3 and 4 that, for almost all the chromophores, two excited states are responsible for the appearance of the lowest energy intense absorption band, the H → L transition being the predominant one thereby indicating a $\pi \rightarrow \pi^*$ intramolecular charge transfer (ICT) from donor molecular orbitals to acceptor (pyridine) molecular orbitals. Thus, from computation, we can predict that as the conjugation length in the chromophores increases (e.g., **17** vs **19** and **18** vs **20**), the HOMO gets destabilized and the HOMO–LUMO gap decreases thereby shifting the absorption maxima bathochromically (see Table 4). Also, in going from **19** to **21** to **22**, it is observed that destabilization of the HOMO by 0.069 and 0.051 eV respectively and a shrinking of the HOMO–LUMO gaps by 0.04 and 0.06 eV respectively indicate the trend in observed absorption in these compounds. However, the experimentally found hypsochromic shift in λ_{abs} of compound **22** could not be explained on the basis of computation.

Potential of the Present System: Asymmetric versus Symmetric. An important parameter for the comparison of photophysical performances of diverse fluorophores is the fluorescence quantum yield (Φ_{em}), which is the direct measure of the efficiency of the conversion of absorbed light into emitted light. We have already shown (in Table 2) that the asymmetrical bipyridines (present work) perform better than corresponding symmetrical bipyridines[15] as far as measured quantum yields are concerned. Thus, as shown in Table 2, the present asymmetrical molecules are more efficient fluorophores than the symmetrical ones.[15] In MeCN solvent, the trend of better photophysical efficiencies of asymmetric bipyridines over symmetrical bipyridines is consistent (Table 2).

In the comparison of symmetry versus asymmetry, the symmetrical fluorophores[15] are larger than their corresponding asymmetrical ones by "one side substituent" of the central bipyridine unit (see Chart 1 and ref 15). In other words, the asymmetrical bipyridines (present work) are of lower molecular weights in comparison to their corresponding symmetrical ones. It would be thus comparatively easier to crystallize the asymmetrical bipyridines into their single crystals, as we have unambiguously characterized the crystal structure of fluorophore **18** as a representative one (vide supra) from this asymmetrical series. Despite our enormous efforts, we could not succeed in crystallizing the corresponding symmetrical bipyridines into their single crystals.[15]

In recent time, there has been a rapid increase in research activity in Ru(II)–bipyridine coordination complexes as efficient photosensitizers in making dye-sensitized solar cells (DSSCs) because of their low-lying metal ligand charge transfer (MLCT) transition that can cover the red and near-infrared region of the solar spectrum. Obtaining an optimal photosensitizer, with an electronic absorption band extending up to red region of the visible spectrum and high molar extinction coefficient, is a challenging task in the area of visible light induced photocatalytic reactions including water oxidation[21] as well as dye-sensitized solar cells.[22] A recent report on 4,4′-unsymmetrically substituted 2,2′-bipyridine Ru(II) coordination complexes demonstrates an improvement in the molar extinction coefficient of all these sensitizers because of the presence of π-conjugation in this system.[23] Thus, the present work dealing with a new series of asymmetrically substituted and π-conjugated 2,2′-bipyridine derivatives demonstrates that these asymmetrical bipyridines have potential to form efficient photosensitizers (for example, with Ru^{2+} ion) in the context of better/improved dye-sensitized solar cells and photocatalytic water splitting.

■ CONCLUSION

In conclusion, a new family of 4-methyl-4′-π-conjugated-2,2′-bipyridine derivatives with A–A–π–D architecture have been designed and accomplished successfully. This system consists of

DOI: 10.1021/acs.joc.5b02345
J. Org. Chem. XXXX, XXX, XXX–XXX

Table 3. Energies of Four Higher Occupied (H−3, H−2, H−1, H) and Four Lower Virtual (L, L+1, L+2, L+3) Molecular Orbitals of the Studied Systems as Computed in CAM-B3LYP/6-31g(d,p) Level Theory (in DCM)[a]

	H−3	H−2	H−1	H	L	L+1	L+2	L+3
16	−8.367	−8.034	−7.765	−6.184	−0.404	−0.100	−0.973	−1.356
17	−7.885	−7.766	−7.451	−6.139	−0.460	−0.067	−0.986	−1.468
18	−7.877	−7.747	−7.441	−5.943	−0.413	−0.101	−0.985	−1.538
19	−7.824	−7.456	−7.107	−6.013	−0.848	−0.052	−0.457	−0.993
20	−7.818	−7.442	−7.067	−5.818	−0.820	−0.027	0.502	1.005
21	−7.810	−7.577	−6.848	−5.944	−0.817	−0.005	0.576	1.028
22	−7.556	−7.399	−6.764	−5.893	−0.824	−0.020	0.522	1.012
23	−7.540	−7.385	−6.711	−5.718	−0.796	0.000	0.566	1.029

[a]H = HOMO, L = LUMO.

Table 4. TD-DFT Computed CAM-B3LYP/6-31g(d,p) Representative Intense Vertical Excitations, λ_{max} and Oscillator Strength (f) of the Synthesized Molecules in DCM

molecule	transition	λ_{max} (nm)	oscillator strength
16	H → L	340.86	1.4844
	H−1 → L	253.78	0.4862
17	H → L	356.47	1.2090
	H−2 → L	255.16	0.4780
	H−2 → L+1	271.32	0.1129
18	H → L	367.76	1.2906
	H−2 → L	255.65	0.4790
19	H → L	382.84	2.0977
	H−1 → L	301.29	0.2137
	H−3 → L	267.55	0.3201
20	H → L	393.36	2.0774
	H−1 → L	274.95	0.2555
21	H → L	393.29	2.0874
	H−3 → L	264.04	0.3902
22	H → L	400.15	2.0030
	H−4 → L	268.68	0.3262
	H → L+2	273.41	0.1410
23	H → L	409.12	2.0238
	H−3 → L	275.24	0.3245

the 2,2-bipyridine heterocycle acting as the acceptor and the fragment containing different donor functionalities. All the chromophores are administered by the intramolecular charge transfer from the donors to the acceptor units. The emissive behavior of all the chromophores has been demonstrated with four of the compounds showing solid-state emission that provides a doorway for solid-state lighting processes. In addition, the title compounds show large solvent sensitive emissive behavior and their photophysical properties of the compounds are highly reliant on the number, nature, and position of the donor functionalities, which have also been computationally corroborated by DFT calculations. In our previous article, we reported symmetrical derivatives of 2,2′-bipyridine, and herein, we report the unsymmetrical derivatives of 2,2′-bipyridine. Thus, a complete library of compounds have been designed and synthesized, and we strongly believe that the unsymmetrical bipyridine derivatives along with their transition metal complexes may also exhibit interesting nonlinear optical behavior. This work is currently being undertaken in our laboratory.

EXPERIMENTAL SECTION

General Procedures. All reactions were carried out under ambient conditions unless otherwise stated. Column chromatography was performed on silica gel (100−200 mesh). TLC plates were visualized in an iodine chamber (sometimes in a UV chamber). Unless stated otherwise, all reagents were purchased from commercial sources and used without additional purification. THF was freshly distilled over Na-benzophenone ketyl. Unless stated otherwise, ^{1}H NMR and ^{13}C NMR spectra were recorded either on a 400 or on a 100 mHz machine in $CDCl_3$ as solvent with TMS as reference. CHNS analyzer has been used for elemental analyses. Infrared (IR) spectra were recorded by using KBr pellets on an FT/IR spectrometer. HRMS (ESI-TOF) equipment was used to record mass spectra for all the title compounds. Absorbance spectra were recorded on a UV−visible spectrophotometer, and fluorescence emission spectra were recorded on a spectrofluorimeter.

Crystallography. Single crystal X-ray diffraction data of compound **18** was measured at room temperature on a single crystal X-ray diffratometer [λ (Mo Kα) = 0.7103 Å] with a graphite monochromator. 2400 frames were recorded with an ω scan width of 0.3°, each for 10 s, and crystal−detector distance of 60 mm with collimator of 0.5 mm.[24] Data reduction was performed with the SAINTPLUS software.[24a] Absorption correction was made using an empirical method SADABS.[24b] Structure solution was performed using the SHELXS-97 program,[24c] and it was refined using the SHELXL-97 program.[24d] Hydrogen atoms on the aromatic rings were introduced on calculated positions and included in the refinement riding on their respective parent atoms. CCDC 1430463 contains the supplementary crystallographic data of compound **18**. Relevant crystal data can be obtained free of charge via http://www.ccdc.cam.atc.uk/conts/retrieving.html, or from the Cambridge Crystallographic Data Centre, 12 Union Road, Cambridge CB2 1EZ, U.K.; fax, (+44) 1223-336-033; or via e-mail, deposit@ccdc.cam.ac.uk.

*Synthesis of (E)-4-Methyl-4′-(4-(pyrrolidin-1-yl)styryl)-2,2′-bipyridine (**16**).* In the presence of nitrogen atmosphere, potassium *tert*-butoxide (0.22 g, 2 mmol) was added at 0 °C to a solution of monophosphonate (**2**, 0.320 g, 1 mmol) and the aldehyde (**7a**, 0.175 g, 1 mmol) in 20 mL of THF; the ice bath was subsequently removed, and the reaction mixture was stirred at room temperature for 1 h. After the completion of the reaction, the reaction mixture was quenched with 10 mL of water, and the product was extracted with dichloromethane. The resulting mixture was washed several times with water and then with brine. The yellow colored material obtained was washed with ether, dried in air, and then further purified on a silica gel (100−200 mesh) column using methanol/dichloromethane 5:95 v/v as the eluent to obtain the compound **16** as a dark brown colored solid. Yield: 0.23 g (72%). IR spectrum (ν/cm^{-1}): 2970, 2926, 1738, 1366, 1229, 1217. ^{1}H NMR (400 MHz, $CDCl_3$): δ 8.56 (d, J = 5 Hz, 2H), 8.46 (s, 1H), 8.27 (s, 1H), 7.45 (d, J = 9 Hz, 2H), 7.40 (d, J = 16 Hz, 1H), 7.33 (d, J = 4 Hz, 1H), 7.15 (d, J = 5 Hz, 1H), 6.89 (d, J = 16 Hz, 1H), 6.56 (d, J = 9 Hz, 2H), 3.33 (t, J = 6 Hz, 4H), 2.45 (s, 3H), 2.02 (t, J = 6 Hz, 4H). ^{13}C NMR (100 MHz, $CDCl_3$): δ 155.1, 155.0, 148.1, 147.8, 147.2, 147.1, 145.9, 132.9, 127.5 (2C), 123.6, 122.5, 121.0, 119.5, 119.4, 116.7, 110.7 (2C), 46.5 (2C), 24.4 (2C), 20.1.

DOI: 10.1021/acs.joc.5b02345
J. Org. Chem. XXXX, XXX, XXX−XXX

HRMS (ESI/TOF-Q) m/z: $(M + H)^+$, calcd for $C_{23}H_{24}N_3$ 342.1970, found 342.1970. Anal. Calcd for $C_{23}H_{23}N_3$: C, 80.90; H, 6.79; N, 12.30. Found: C, 80.72; H, 6.71; N, 12.41.

*Synthesis of (E)-N,N-Dibutyl-2,5-dimethoxy-4-(2-(4′-methyl-2,2′-bipyridin-4-yl)vinyl)aniline (**17**).* The monophosphonate (**2,** 0.32 g, 1 mmol) and the aldehyde (**5b**, 0.29 g, 1 mmol) were dissolved in 20 mL of dry THF. Then, potassium *tert*-butoxide (0.224 g, 2 mmol) was added to the reaction mixture at 0 °C under nitrogen atmosphere; ice bath was then removed and stirred at room temperature for 1 h. The resulting dark colored solution was quenched with 10 mL of water, and the product was extracted with dichloromethane. The organic layer was washed several times with water and with brine and dried over Na_2SO_4, and the crude product was purified by column chromatography using silica gel (100−200 mesh) using methanol/dichloromethane 5:95 v/v as the eluent to obtain compound **17**, which is a dark red colored thick gum. Yield: 0.36 g (78%). IR spectrum (ν/cm^{-1}): 2953, 2928, 2859, 1585, 1504, 1460, 1204, 1040, 965, 819. ^{1}H NMR (400 MHz, $CDCl_3$): δ 8.59 (d, J = 5 Hz, 1H), 8.56 (d, J = 5 Hz, 1H), 8.45 (s, 1H), 8.24 (s, 1H), 7.73 (d, J = 16 Hz, 1H), 7.40 (d, J = 5 Hz, 1H), 7.13 (d, J = 5 Hz, 1H), 7.07 (s, 1H), 7.02 (d, J = 16 Hz, 1H), 6.48 (s, 1H), 3.86 (s, 6H), 3.17 (t, J = 8 Hz, 4H), 2.43 (s, 3H), 1.50 (quin, J = 8 Hz, 4H), 1.34 (sextet, J = 8 Hz, 4H), 0.90 (t, J = 7 Hz, 6H). ^{13}C NMR (100 MHz, $CDCl_3$): δ 156.4, 156.1, 152.4, 149.2, 148.9, 148.1, 147.0, 146.8, 142.2, 128.1, 124.6, 123.6, 122.0, 120.3, 118.4, 117.3, 110.8, 104.5, 56.2 (2C), 52.2 (2C), 29.3 (2C), 21.2, 20.5 (2C), 14.0 (2C). HRMS (ESI/TOF-Q) m/z: $(M + H)^+$, calcd for $C_{29}H_{38}N_3O_2$ 460.2964, found 460.2963. Anal. Calcd for $C_{29}H_{37}N_3O_2$: C, 75.78; H, 8.11; N, 9.14. Found: C, 75.62; H, 8.15; N, 9.23.

*Synthesis of (E)-4-(2,5-Dimethoxy-4-(pyrrolidin-1-yl)styryl)-4′-methyl-2,2′-bipyridine (**18**).* This compound was synthesized using the same pathway as described for compound **17**. Aldehyde **7b** (0.26 g, 1 mmol) was used instead of aldehyde **5b**. That resulting dark gray colored solid was subjected to chromatographic purification over silica gel (100−200 mesh) using methanol/dichloromethane 5:95 v/v as the eluent to obtain the compound **18** as a brown colored solid. The compound was isolated as brown colored single crystals. Yield: 0.30 g (76%). ^{1}H NMR (400 MHz, $CDCl_3$): δ 8.55 (t, J = 5 Hz, 2H), 8.42 (s, 1H), 8.22 (s, 1H), 7.72 (d, J = 16 Hz, 1H), 7.37 (d, J = 5 Hz, 1H), 7.09 (d, J = 5 Hz, 1H), 7.05 (s, 1H), 6.93 (d, J = 16 Hz, 1H), 6.21 (s, 1H), 3.83 (s, 3H), 3.79 (s, 3H), 3.39 (t, J = 6 Hz, 4H), 2.40 (s, 3H), 1.90 (t, J = 6 Hz, 4H). ^{13}CNMR (100 MHz, $CDCl_3$): δ 156.2, 156.0, 153.2, 149.0, 148.8, 148.0, 147.2, 143.7, 141.7, 128.3, 124.6, 122.0, 121.8, 120.1, 118.28, 114.1, 111.3, 98.9, 56.8, 56.1, 50.4(2C), 25.2(2C), 21.1. HRMS (ESI/TOF-Q) m/z: $(M + H)^+$, calcd for $C_{25}H_{28}N_3O_2$ 402.2182, found 402.2181. Anal. Calcd for $C_{25}H_{27}N_3O_2$: C, 74.79; H, 6.78; N, 10.47. Found: C, 74.85; H, 6.71; N, 10.36.

*Synthesis of N,N-Dibutyl-2,5-dimethoxy-4-(4-((E)-2-(4′-methyl-2,2′-bipyridin-4-yl)vinyl)styryl)aniline (**19**).* Synthesis of this compound follows the same procedure as described for **17**. Aldehyde **11b** (0.19 g, 1 mmol) was used instead of aldehyde **5b**. The crude product was purified through column chromatography using silica gel (100−200 mesh) and methanol/dichloromethane 5:95 v/v as mobile phase to obtain compound **19** as a thick dark red gum. Yield: 0.22 g (80.%). IR spectrum (ν/cm^{-1}): 2953, 2925, 2853, 1721, 1587, 1501, 1458, 1373, 1205, 1042, 960, 824. ^{1}H NMR (400 MHz, $CDCl_3$): δ 8.62 (d, J = 5 Hz, 1H), 8.57 (d, J = 5 Hz, 1H), 8.51 (s, 1H), 8.26 (s, 1H), 7.53 (s, 4H), 7.79 (d, J = 16 Hz, 1H), 7.43 (d, J = 16 Hz, 1H), 7.36 (d, J = 5 Hz, 1H), 7.14 (d, J = 5 Hz, 1H), 7.12 (t, 2H), 6.99 (d, J = 16 Hz, 1H), 6.51 (s, 1H), 3.87 (s, 3H), 3.86 (s, 3H), 3.16 (t, J = 7 Hz, 4H), 2.44 (s, 3H), 1.50 (quin, J = 7 Hz, 4H), 1.33−1.28 (m, 4H), 0.90 (t, J = 7 Hz, 6H). ^{13}C NMR (100 MHz, $CDCl_3$): δ 156.6, 155.9, 151.8, 149.4, 148.9, 148.2, 147.4, 145.8,141.3, 138.9, 134.7, 133.0, 127.3, 126.6, 125.6, 125.3, 1254.8, 123.9, 122.0, 120.9, 118.7, 118.1, 110.3, 105.2, 56.5, 56.3, 52.3 (2C), 29.3 (2C), 21.2, 20.5 (2C), 14.0 (2C). HRMS (ESI/TOF-Q) m/z: $(M + H)^+$, calcd for $C_{37}H_{44}N_3O_2$ 562.3434, found 562.3432. Anal. Calcd for $C_{37}H_{43}N_3O_2$: C, 79.11; H, 7.72; N, 7.48. Found: C, 79.03; H, 7.82; N, 7.36.

*Synthesis of 4-(4-(2,5-Dimethoxy-4-(pyrrolidin-1-yl)styryl)styryl)-4′-methyl-2,2′-bipyridine (**20**).* Synthesis of this compound follows the same procedure as described for **17**. Aldehyde **12b** (0.37 g, 1 mmol) was used instead of aldehyde 7**b**. The crude product was further purified on a silica gel (100−200 mesh) column using methanol/dichloromethane 5:95 v/v as the eluent to obtain the compound **20**, which was isolated as gray microcrystalline solid. Yield: 0.39 g (77%). IR spectrum (ν/cm^{-1}): 2947, 2934, 2926, 1736, 1586, 1519, 1453, 1359, 1209, 1040, 963, 825. ^{1}H NMR (400 MHz, $CDCl_3$): δ 8.63 (d, J = 5 Hz, 1H), 8.58 (d, J = 5 Hz, 1H), 8.52 (s, 1H), 8.26 (s, 1H), 7.53 (s, 4H), 7.48 (d, J = 13 Hz, 1H), 7.44 (d, J = 13 Hz, 1H), 7.38 (d, J = 6 Hz, 1H), 7.16 (d, J = 4 Hz, 1H), 7.10 (t, J = 13 Hz 2H), 6.93 (d, J = 16 Hz, 1H), 6.31 (s, 1H), 3.87 (s, 3H), 3.85 (s, 3H), 3.41 (t, J = 6 Hz, 4H), 2.46 (s, 3H), 1.96 (t, J = 6 Hz, 4H). ^{13}C NMR (100 MHz, $CDCl_3$): δ 156.5, 155.9, 152.6, 149.4, 148.9, 148.1, 145.9, 144.0, 141.0, 139.2, 134.4, 133.1, 127.4, 126.4, 125.1, 124.8, 124.1, 122.0, 120.8, 118.1, 115.5, 110.7, 99.54, 56.9, 56.3, 50.4 (2C), 25.1 (2C), 21.2. HRMS (ESI/TOF-Q) m/z: $(M + H)^+$, calcd for $C_{33}H_{34}N_3O_2$ 504.2651, found 504.2650. Anal. Calcd for $C_{33}H_{33}N_3O_2$: C, 78.70; H, 6.60; N, 8.34. Found: C, 78.64; H, 6.71; N, 8.26.

*Synthesis of N,N-dibutyl-4-(2,5-dibutoxy-4-((E)-2-(4′-methyl-2,2′-bipyridin-4-yl)vinyl)styryl)aniline (**21**).* Synthesis of this compound follows same procedure as described for **17**. Aldehyde **13b** (0.24 g, 1 mol) was used instead of aldehyde **5b**. The dark brown crude was purified on a silica gel (100−200 mesh) column using methanol/dichloromethane 5:95 v/v as the eluent to obtain the compound **21** as dark brown solid. Yield: 0.33 g (56%). IR spectrum (ν/cm^{-1}): 2956, 2924, 2855, 1721, 1589, 1519, 1462, 1368, 1201, 1187, 1067, 968, 821. ^{1}H NMR (400 MHz, $CDCl_3$): δ 8.55 (d, J = 5 Hz, 1H), 8.49 (d, J = 4 Hz, 1H), 8.39 (s, 1H), 8.17 (s, 1H), 7.69 (d, J = 16 Hz, 1H), 7.35 (d, J = 6 Hz, 2H), 7.32 (s, 1H), 7.19 (s, 1H), 7.13 (d, J = 16 Hz, 1H), 7.08−6.98 (m, 4H), 6.56 (d, J = 8 Hz, 2H), 4.02 (t, J = 6 Hz,2H), 3.97 (t, J = 6 Hz, 2H), 3.22 (t, J = 7 Hz, 4H), 2.38 (s, 3H), 1.80 (sextet, J = 7 Hz, 4H), 1.52 (quin, J = 7 Hz, 8H), 1.29 (sextet, J = 7 Hz, 4H), 0.99−0.94 (m, 6H), 0.89 (t, J = 7 Hz, 6H). ^{13}C NMR (100 MHz, $CDCl_3$): δ 156.6, 156.0, 151.7, 150.5, 149.3, 148.9, 148.1, 147.8, 146.6, 129.7, 129.4, 128.4, 127.9, 125.6, 125.0, 124.7, 124.3, 122.0, 120.2, 118.9, 118.1, 111.6, 111.2, 109.9, 69.2, 69.1, 50.8 (2C), 31.6, 31.5, 29.5, 21.2, 20.3 (2C), 19.5, 19.4, 14.0, 13.9 (2C). HRMS (ESI/TOF-Q) m/z: $(M + H)^+$, calcd for $C_{43}H_{56}N_3O_2$ 645.4373, found 646.4377. Anal. Calcd for $C_{43}H_{55}N_3O_2$: C, 79.96; H, 8.58; N, 6.51. Found: C, 79.85; H, 8.62; N, 6.45.

*Synthesis of N,N-Dibutyl-4-(2,5-dibutoxy-4-((E)-2-(4′-methyl-2,2′-bipyridin-4-yl)vinyl)styryl)-2,5-dimethoxyaniline (**22**).* This compound was synthesized by same procedure as described for **16.** Aldehyde **14b** (0.53 g, 1 mmol) was used instead of aldehyde **5b**. The resultant dark red colored crude product was purified by a silica gel column (100−200 mesh) eluting with methanol/dichloromethane in 5:95 v/v as mobile phase. The compound **22** was isolated as a dark red gum. Yield: 0.48 g (69%). IR spectrum (ν/cm^{-1}): 2955, 2924, 2854, 1734, 1588, 1505, 1463, 1377, 1202, 1042, 968, 853. ^{1}H NMR (400 MHz, $CDCl_3$): δ 8.62 (d, J = 5 Hz, 1H), 8.55 (d, J = 5 Hz, 1H), 8.46 (s, 1H), 8.23 (s, 1H), 7.77 (d, J = 16 Hz, 1H), 7.48 (d, J = 16 Hz, 1H), 7.41 (t, 1H), 7.36 (d, J = 16 Hz, 1H), 7.16 (t, J = 13 Hz, 2H), 7.12 (d, J = 4 Hz, 3H), 6.55 (s, 1H), 4.08 (t, J = 6 Hz, 2H), 4.05 (t,, J = 6 Hz, 2H), 3.85 (d, J = 5 Hz, 6H), 3.17 (t, J = 8 Hz 4H), 2.42 (s, 3H), 1.89−1.82 (m, 4H), 1.60 (quin,, J = 7 Hz, 4H), 1.53−1.45(m, 4H), 1.34−1.28 (m, 4H), 1.03 (m, 6H), 0.91(t, J = 7 Hz, 6H). ^{13}C NMR (100 MHz, $CDCl_3$): δ 156.5, 155.9, 151.76, 151.71, 150.7, 149.2, 148.9 (2C), 148.2, 147.5, 146.6, 129.3, 128.4, 125.8, 124.7 (2C), 123.9, 122.12C), 121.2, 120.3, 118.9, 111.2, 110.4, 110.3, 105.5, 69.1 (2C), 56.5, 56.2, 52.5 (2C), 31.6, 31.5, 29.9 (2C), 21.1, 20.5, 19.5 (2C), 14.0 (3C). HRMS (ESI/TOF-Q) m/z: $(M + H)^+$, calcd for $C_{45}H_{60}N_3O_4$ 706.4584, found 706.4585. Anal. Calcd for $C_{45}H_{59}N_3O_4$: C, 76.56; H, 8.42; N, 5.95. Found: C, 76.65; H, 8.36; N, 5.85.

*Synthesis of 4-(2,5-Dibutoxy-4-(2,5-dimethoxy-4-(pyrrolidin-1-yl)styryl)styryl)-4′-methyl-2,2′-bipyridine (**23**).* This compound was synthesized following the same procedure for **17**. Aldehyde **15b** (0.24 g, 1 mmol) was used instead of aldehyde **5b**. The crude product was purified through column chromatography using silica gel (100−200 mesh) and methanol/dichloromethane 5:95 v/v as mobile phase to obtain compound **23** as a dark red microcrystalline solid. Yield: 0.22 g (71%). IR spectrum (ν/cm^{-1}): 2958, 2928, 1737, 1712, 1587, 1452,

DOI: 10.1021/acs.joc.5b02345
J. Org. Chem. XXXX, XXX, XXX−XXX

1357, 1217, 1117, 1040, 970, 821. ^{1}H NMR (400 MHz, $CDCl_3$): δ 8.64 (d, J = 5 Hz, 1H), 8.58 (d, J = 5 Hz, 1H), 8.50 (s, 1H), 8.27 (s,1H), 7.65 (d, J = 17 Hz, 1H), 7.49 (d, J = 16 Hz, 1H), 7.43 (d, J = 5 Hz, 1H), 7.39 (d, J = 16 Hz, 1H), 7.19 (t, 3H), 7.13 (d,J = 5 Hz, 2H), 6.30 (s,1H), 4.11 (t, J = 6 Hz, 2H), 4.07 (t, J = 6 Hz, 2H), 3.88 (s, 3H), 3.86 (s, 3H), 3.42 (t, J = 7 Hz, 4H), 2.46 (s, 3H), 1.97 (unresolved, 4H), 1.96−1.87 (m, 4H), 1.65−1.59 (m, 4H), 1.06 (q, J = 7 Hz, 6H). ^{13}C NMR (100 MHz, $CDCl_3$): δ 156.6, 156.0, 152.5, 151.7, 150.6, 149.3, 148.9, 148.1, 146.6, 144.1, 140.8, 129.7, 128.4, 125.6, 124.7, 124.4, 124.1, 122.0, 120.2, 119.5, 118.9, 116.5, 111.3, 110.8, 110.1, 99.8, 69.3, 69.2, 56.8, 56.5, 50.4 (2C), 31.67, 31.5, 25.09 (2C), 21.2, 19.5 (2C), 14.0 (2C). HRMS (ESI/TOF-Q) m/z: $(M + H)^+$, calcd for $C_{41}H_{50}N_3O_4$ 648.3801, found 648.3807. Anal. Calcd for $C_{41}H_{49}N_3O4$: C, 76.01; H, 7.62; N, 6.49. Found: C, 76.12; H, 7.71; N, 6.58.

■ ASSOCIATED CONTENT

Supporting Information

The Supporting Information is available free of charge on the ACS Publications website at DOI: 10.1021/acs.joc.5b02345.

X-ray crystallographic data for **18** (CIF)

Synthesis schemes, NMR and optical spectra, HRMS and CHNS analysis plots, and computational details (PDF)

■ AUTHOR INFORMATION

Corresponding Author

*E-mail: skdas@uohyd.ac.in; samar439@gmail.com. Phone: +91 40 2301 1007. Fax: +91 40 2301 2460.

Notes

The authors declare no competing financial interest.

■ ACKNOWLEDGMENTS

We thank Science & Engineering Research Board (a statutory body under the Department of Science and Technology), Government of India, for financial support (Project No. SB/SI/IC/034/2013). The 400 MHz NMR facilities at University of Hyderabad by DST, Government of India, is gratefully acknowledged. We acknowledge high performance computational facility at the Centre for Modeling, Simulation and Design (CMSD), University of Hyderabad Campus. We thank Mrs. Asia Perwez for helping us to record the mass HRMS spectra of compounds **16**−**23**. R.B. thanks UGC, India, respectively for his fellowship. Single crystal X-ray diffraction facility at University of Hyderabad by DST, Government of India, is acknowledged. Our special thanks to Mr. Krishnachari for helping us with quantum yield calculations. We are grateful to Prof. S. Mahapatra, School of Chemistry, University of Hyderabad, for giving us helpful suggestions in connection with DFT calculations.

■ REFERENCES

(1) (a) Chen, S.; Xu, X.; Liu, Y.; Yu, G.; Sun, X.; Qiu, W.; Ma, Y.; Zhu, D. *Adv. Funct. Mater.* **2005**, *15*, 1541−1546. (b) Mondal, E.; Hung, W.-Y.; Dai, H.-C.; Wong, K.-T. *Adv. Funct. Mater.* **2013**, *23*, 3096−3105.

(2) Abbotto, A.; Beverina, L.; Bozio, R.; Facchetti, A.; Ferrante, C.; Pagani, G. A.; Pedron, D.; Signorini, R. *Chem. Commun.* **2003**, 2144−2145.

(3) Lai, R. Y.; Fabrizio, E. F.; Lu, L.; Jenekhe, S. A.; Bard, A. J. *J. Am. Chem. Soc.* **2001**, *123*, 9112−9118.

(4) Wong, M. S.; Li, Z. H.; Tao, Y.; D'Iorio, M. *Chem. Mater.* **2003**, *15*, 1198−1203.

(5) (a) Jiao, G. S.; Thoresen, L. H.; Burgess, K. *J. Am. Chem. Soc.* **2003**, *125*, 14668−14669. (b) Sreejith, S.; Divya, K. P.; Ajayaghosh, A. *Chem. Commun.* **2008**, 2903−2905. (c) Ajayaghosh, A.; Carol, P.; Sreejith, S. *J. Am. Chem. Soc.* **2005**, *127*, 14962−14963. (d) Divya, K. P.; Sreejith, S.; Balakrishna, B.; Jayamurthy, P.; Anees, P.; Ajayaghosh, A. *Chem. Commun.* **2010**, *46*, 6069−6071.

(6) Cariati, E.; Pizzotti, M.; Roberto, D.; Tessore, F.; Ugo, R. *Coord. Chem. Rev.* **2006**, *250*, 1210−1233.

(7) Mazzucato, S.; Fortunati, I.; Scolaro, S.; Zerbetto, M.; Ferrante, C.; Signorini, R.; Pedron, D.; Bozio, R.; Locatelli, D.; Righetto, S.; Roberto, D.; Ugo, R.; Abbotto, A.; Archetti, G.; Beverina, L.; Ghezzi, S. *Phys. Chem. Chem. Phys.* **2007**, *9*, 2999−3005.

(8) Zyss, J.; Ledoux, I. *Chem. Rev.* **1994**, *94*, 77−105.

(9) (a) Aubert, V.; Guerchais, V.; Ishow, E.; Hoang-Thi, K.; Ledoux, I.; Nakatani, K.; Le Bozec, H. *Angew. Chem., Int. Ed.* **2008**, *47*, 577−580. (b) Berner, D.; Klein, C.; Nazeeruddin, M. K.; De Angelis, F.; Castellani, M.; Bugnon, P.; Scopelliti, R.; Zuppiroli, L.; Graetzel, M. *J. Mater. Chem.* **2006**, *16*, 4468−4474. (c) Klein, C.; Baranoff, E.; Nazeeruddin, Md. K.; Grätzel, M. *Tetrahedron Lett.* **2010**, *51*, 6161−6165. (d) Aubert, V.; Ishow, E.; Ibersiene, F.; Boucekkine, A.; Williams, J. A. G.; Toupet, L.; Métivier, R.; Nakatani, K.; Guerchais, V.; Le Bozec, H. *New J. Chem.* **2009**, *33*, 1320−1323. (e) Araya, J. C.; Gajardo, J.; Moya, S. A.; Aguirre, P.; Toupet, L.; Williams, J. A. G.; Escadeillas, M.; Le Bozec, H.; Guerchais, V. *New J. Chem.* **2010**, *34*, 21−24.

(10) Sandroni, M.; Favereau, L.; Planchat, A.; Akdas-Kilig, H.; Szuwarski, N.; Pellegrin, Y.; Blart, E.; Le Bozec, H.; Boujtita, M.; Odobel, F. *J. Mater. Chem. A* **2014**, *2*, 9944−9947.

(11) Dragonetti, C.; Colombo, A.; Marinotto, D.; Righetto, S.; Roberto, D.; Valore, A.; Escadeillas, M.; Guerchais, V.; Le Bozec, H.; Boucekkine, A. *J. Organomet. Chem.* **2014**, *751*, 568−572.

(12) Le Bozec, H.; Guerchais, V. *C. R. Chim.* **2013**, *16*, 1172−1182.

(13) Nair, M. N.; Hobeika, N.; Calard, F.; Malval, J.-P.; Aloıse, S.; Spangenberg, A.; Simon, L.; Cranney, M.; Vonau, F.; Aubel, D.; Serein-Spirau, F.; Lere-Porte, J.-P.; Lacour, M.-G.; Jarrosson, T. *Phys. Chem. Chem. Phys.* **2014**, *16*, 12826−12837.

(14) Xu, D.; Yu, Z.; Yang, M.; Zheng, Z.; Zhu, L.; Zhang, X.; Ye, L.; Wu, J.; Tian, Y.; Zhou, H. *Dyes Pigm.* **2014**, *100*, 142−149.

(15) Sarma, M.; Chatterjee, T.; Ghanta, S.; Das, S. K. *J. Org. Chem.* **2012**, *77*, 432−444.

(16) Dorta, R.; Shimon, L. J. W.; Rozenberg, H.; Ben-David, Y.; Milstein, D. *Inorg. Chem.* **2003**, *42*, 3160−3167.

(17) Smith, A. P.; Fraser, C. L. *Comprehensive Coordination Chemistry II.* **2003**, *1*, 1−23.

(18) Bourgault, M.; Renouard, T.; Lognoné, B.; Mountassir, C.; Bozec, H. L. *Can. J. Chem.* **1997**, *75*, 318−325.

(19) (a) Lu, X.; Fan, S.; Wu, J.; Jia, X.; Wang, Z.-S.; Zhou, G. *J. Org. Chem.* **2014**, *79*, 6480−6489. (b) Soujanya, T.; Philippon, A.; Leroy, S.; Vallier, M.; Fages, F. *J. Phys. Chem. A* **2000**, *104*, 9408−9414.

(20) Frisch, M. J.; et al. *Gaussian 09, revision B.01*; Gaussian, Inc.: Wallingford, CT, 2010.

(21) Duan, L.; Xu, Y.; Zhang, P.; Wang, M.; Sun, L. *Inorg. Chem.* **2010**, *49*, 209−215.

(22) Yang, S.-H.; Wu, K.-L.; Chi, Y.; Cheng, Y.-M.; Chou, P.-T. *Angew. Chem., Int. Ed.* **2011**, *50*, 8270−8274.

(23) Chandrasekharam, M.; Kumar, CH. P.; Singh, S. P.; Anusha, V.; Bhanuprakash, K.; Islam, A.; Han, L. *RSC Adv.* **2013**, *3*, 26035−26046.

(24) (a) *Software for the CCD Detector System*; Bruker Analytical X-Ray Systems, Inc.: Madison, WI, 1998. (b) Sheldrick, G. M. *SADABS, Program for Absorption Correction with the Siemens SMART Area-Detector System*; University of Gottingen: Gottingen, Germany, 1996. (c) Sheldrick, G. M. *SHELXS-97, Program for Solution of Crystal Structures*; University of Gottingen: Gottingen, Germany, 1997. (d) Sheldrick, G. M. *SHELXL-97, Program for Refinement of Crystal Structures*; University of Gottingen: Gottingen, Germany, 1997.

DOI: 10.1021/acs.joc.5b02345
J. Org. Chem. XXXX, XXX, XXX−XXX